Ab initio simulation studies on the room-temperature ferroelectricity in two-dimensional *β*-phase GeS

Huabing Yin (iD), Chang Liu, Guang-Ping Zheng (iD), Yuanxu Wang (iD), and Fengzhu Ren

View Online   Export Citation   CrossMark

ARTICLES YOU MAY BE INTERESTED IN

Two-dimensional multiferroic semiconductors with coexisting ferroelectricity and ferromagnetism
Applied Physics Letters **113**, 043102 (2018); https://doi.org/10.1063/1.5038037

Promising ferroelectricity in 2D group IV tellurides: a first-principles study
Applied Physics Letters **111**, 132904 (2017); https://doi.org/10.1063/1.4996171

Giant piezoelectricity of monolayer group IV monochalcogenides: SnSe, SnS, GeSe, and GeS
Applied Physics Letters **107**, 173104 (2015); https://doi.org/10.1063/1.4934750

Ab initio simulation studies on the room-temperature ferroelectricity in two-dimensional β-phase GeS

View Online   Export Citation   CrossMark

Huabing Yin,[1,2] Chang Liu,[1] Guang-Ping Zheng,[2,a] Yuanxu Wang,[1,a] and Fengzhu Ren[1]

AFFILIATIONS

[1]Institute for Computational Materials Science, School of Physics and Electronics, Henan University, Kaifeng 475004, China
[2]Department of Mechanical Engineering, The Hong Kong Polytechnic University, Hong Kong 999077, China

[a]Electronic addresses: mmzheng@polyu.edu.hk and wangyx@henu.edu.cn

ABSTRACT

Stable ferroelectricity with an in-plane spontaneous polarization of 2.00×10^{-10} C/m is found in two-dimensional (2D) β-GeS monolayers from theoretical calculations, which can be effectively tuned by the applied tensile strains. The Curie temperature of the monolayer is evaluated to be 358 K by *ab initio* molecular dynamics simulations. Remarkably, the 2D ferroelectricity is found to exist in 2D few-layer β-GeS nanosheets which could be synthesized in experiments. The strong spontaneous polarization and giant pyroelectric coefficient accompanied by the appearance of phase transition near room temperature facilitate the development of β-GeS monolayers or nanosheets for applications in ferroelectric, pyroelectric, and piezoelectric devices with superior performance.

Published under license by AIP Publishing. https://doi.org/10.1063/1.5097425

When the thickness of bulk ferroelectrics is reduced to nanometers, such as $1.2-2.4$ nm for perovskite compounds,[1–3] the unintended depolarization field may lead to the disappearance of ferroelectricity in the material. It is hoped that two-dimensional (2D) layered materials provide a new perspective to retain the functional properties of ferroelectrics when thinned to a few atomic layers,[4,5] and the ferroelectricity is strongly expected to exist in 2D materials. Recently, 2D ferroelectric materials have been reported. In experiments, ferroelectricity has been found to exist in 1-unit cell thick SnTe films and 2D CuInP$_2$S$_6$ films with a Curie temperature (T_c) close to room temperature.[6,7] The ferroelectricity of α-In$_2$Se$_3$ has been found to exhibit the intercorrelated out-of-plane and in-plane polarizations,[8,9] confirming the theoretical predictions. Transformed from β-In$_2$Se$_3$, the β' phase has been discovered to possess an in-plane ferroelectricity stable up to 473 K.[10] Meanwhile, based on theoretical methods, some atom-thick 2D materials, such as $1T$-MoS$_2$,[5] group-IV or III–V binary compounds,[11] α-phase group-IV monochalcogenides,[12] group-IV tellurides,[13] AgBiP$_2$Se$_6$,[14] GaTeCl,[15] β-GeSe,[16] group-V elemental monolayers,[17] and phosphorene-like α-SbN and α-BiP binary monolayers,[18] have been systematically investigated and some of them are found to exhibit amazing ferroelectricity. Remarkably, the *ab initio* molecular dynamics (AIMD) simulation showed that the spontaneous polarization (P_s) of monolayer α-SbN can be retained with the increase in temperature until the melting point, such as 1700 K.[18] In addition, previously reported 2D group-IV

monochalcogenides, including α-SnS, α-GeSe, and α-GeS, with the theoretical P_s of $2.62 \times 10^{-10}-5.06 \times 10^{-10}$ C/m, also exhibit significantly higher T_c than room temperature, i.e., $1200-6400$ K.[12] Such high phase transition temperatures possibly restrict the application of those 2D materials in some practical applications, such as pyroelectric and electrocaloric devices,[19–22] which usually show the best performance around T_c. Normally, it is hoped that those devices could be operated near room temperature. Therefore, the 2D ferroelectric materials with appropriate P_s and T_c are still missing or need to be augmented.

In this letter, using first-principles density functional theory (DFT) together with AIMD simulation, we systematically investigate the ferroelectricity in 2D β-phase GeS, which has the attributes in terms of crystal structure, stacking form, and electronic properties similar to the recently synthesized β-GeSe.[23] All calculations are performed by using the VASP code,[24–26] and the computational details are provided in the supplementary material. Our calculations show that the β-GeS monolayer has a strong in-plane P_s of 2.00×10^{-10} C/m, which is larger than that of monolayer β-GeSe and SnTe and can be enhanced by the applied tensile strains. Meanwhile, its T_c of 358 K predicted by the AIMD simulations is close to room temperature. The ferroelectricity of β-GeS can be maintained in 2D nanosheets with odd numbers of monolayers. In addition, monolayer β-GeS exhibits giant pyroelectric and piezoelectric responses. These extraordinary properties ensure that 2D β-GeS has a wide range of applications in ferroelectric, pyroelectric, and electrocaloric devices.

We focus our attention on the homogeneous monolayer β-GeS, with a space group $Pmn2_1$. Herein, the structural definition of β-phase GeS follows that of β-GeSe recently synthesized in experiments,[23,27] whose structure is exactly identical to that of γ-phase phosphorenelike group-V monolayers.[28–30] More structural descriptions can be found in the supplementary material, and the comparison of the structures of phosphorene and the GeS monolayer is shown in Fig. S1. The optimized conformation of monolayer β-GeS is displayed in Fig. 1(a), whose lattice constants a and b are 5.68 Å and 3.51 Å, respectively, in good agreement with the previously calculated values.[27,31] The phonon spectrum without an appreciable imaginary phonon mode as shown in Fig. 1(b) confirms the thermodynamic stability of monolayer β-GeS. Very similar to β-GeSe, bulk layered β-GeS may be experimentally synthesized from its polymorphs and could be stable under ambient conditions. Meanwhile, its monolayer can be possibly obtained through exfoliation, which is usually used to peel thin flakes from layered bulk crystals, such as graphene and phosphorene.[32,33] As shown in Fig. 1(c), the band structure indicates that monolayer β-GeS is an indirect bandgap material, and both the conduction band minimum (CBM) and the valence band maximum (VBM) are located along the $\Gamma - Y$ line. The energy bandgap in the semilocal PBE functional is about 1.77 eV, which is known to be underestimated considerably. When the HSE hybrid functional is adopted to describe the electronic structure, we obtain a relatively large bandgap of 2.53 eV, close to the GW result of 3.08 eV.[27] It is worth noting that the electronic properties of this category of monolayer β-phase group-IV monochalcogenides have been discussed adequately in previous studies,[27,31] such as the properties of saddle-point excitons.

As shown in Fig. 2(a), phases A, B, and B* indicate an undistorted nonpolar state and two noncentrosymmetric distorted degenerate ferroelectric states of the monolayer, respectively, which were previously well defined in the investigation of ferroelectricity in other similar 2D materials.[12–17] The free-energy contour calculated by DFT
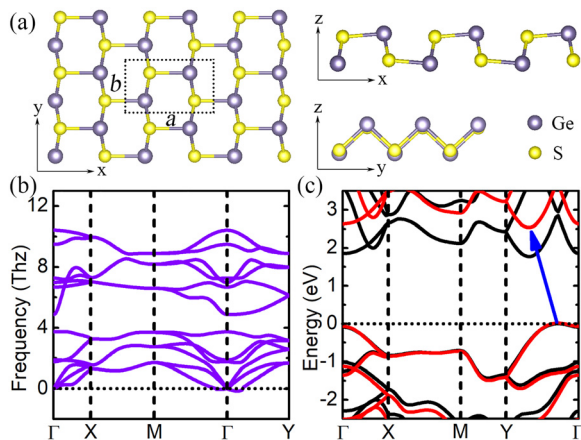

FIG. 2. (a) Two distorted degenerate ferroelectric states (phases B and B*) and an undistorted nonpolar structure (phase A). The in-plane displacements along the x direction of the two nearest neighbor Ge and S atoms are labeled as d_1 and d_2, respectively. Polarization directions are indicated by red arrows. (b) The free-energy contour for β-GeS monolayer vs the x direction displacements d_1 and d_2.

methods vs the x direction displacements of d_1 and d_2 is displayed in Fig. 2(b), manifesting the stable phases B (with $d_1 = d_2 = 0.306$ Å) and B* (with $d_1 = d_2 = -0.306$ Å) with opposite P_s. In a typical polarization reversal process, such as that changed from phase B to phase B*, the reversal path is strictly along the dashed line shown in Fig. 2(b), retaining the relation of $d_1 = d_2$. Therefore, saddle point A between phases B and B* is shaped, corresponding to a centrosymmetric nonpolar state. This double-well free-energy in monolayer β-GeS typically indicates the possibility of its application as ferroelectric materials. Figure 3(a) shows the phonon spectrum of the nonpolar phase A. Compared with that of the distorted polar phase B or B* [see Fig. 1(b)], the phonon spectrum exhibits a prominent imaginary

FIG. 1. (a) Top and side views of the optimized structure of monolayer β-GeS. The armchair and zigzag directions are defined as the x and y directions, respectively. The orthogonal unit cell used in calculations is outlined by dashed lines. (b) Phonon spectrum of monolayer β-GeS. (c) Calculated DFT band structure of monolayer β-GeS by using Perdew-Burke-Ernzerhof (PBE) (black lines) and Heyd-Scuseria-Ernzerhof (HSE) (red lines) functionals, respectively. The blue arrow indicates the position of the HSE bandgap, and the valence band maximum is set at zero energy.
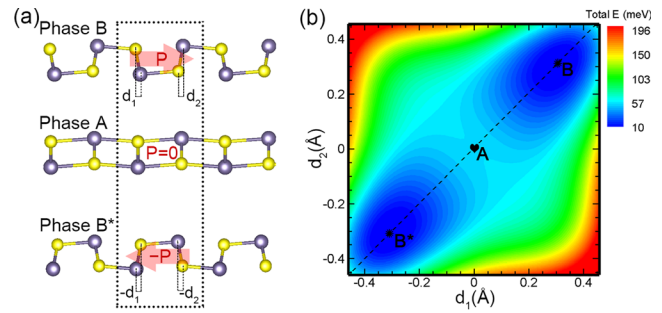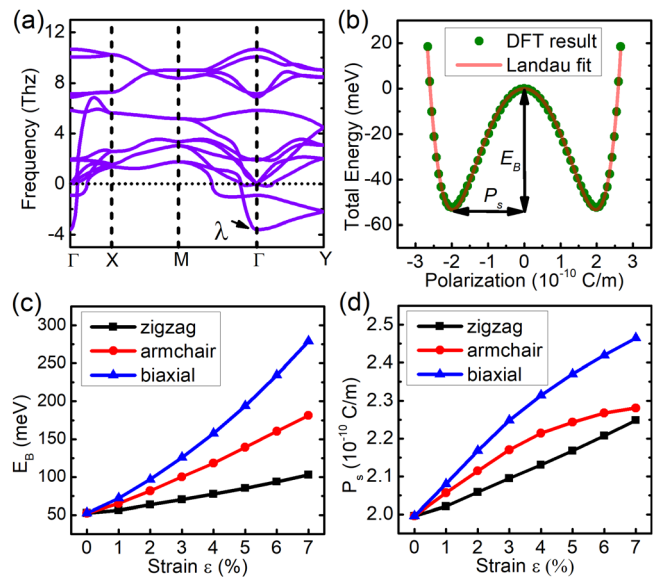

FIG. 3. (a) Phonon spectrum of the centrosymmetric phase A of monolayer β-GeS. (b) Double-well potential vs polarization of monolayer β-GeS. The polarization P_s and potential barrier E_B are all labeled. The fitting curve (red line) is based on the Landau model. (c) E_B and (d) P_s under the applied uniaxial (along the armchair or zigzag direction) and biaxial strains.

frequency of the λ mode at the Γ point for phase A, which is usually a signature of displacive instability and shows a general tendency of the phase transition from a centrosymmetric state to a non-centrosymmetric state below T_c.

As calculated by the Berry phase method (see Fig. S2 in the supplementary material), the in-plane P_s of the β-GeS monolayer is 2.00×10^{-10} C/m along the x axis, which is relatively small compared to that (5.06×10^{-10} C/m) of the α-GeS monolayer,[12] while it is larger than that of the homogeneous β-GeSe monolayer (1.59×10^{-10} C/m).[16] The results can be explained by the correlation between P_s or structure distortions and the chemical bonding nature such as bond covalency and cophonicity, as proposed by Fei et al.[12] Assuming the effective thickness of 4.12 Å for the monolayer,[27] the in-plane P_s value of 0.49 C/m^2 can be estimated for the β-GeS monolayer.

Furthermore, we calculated a series of free energies and polarizations P in the process of phase transition along the displacement-covariant line, $d_1 = d_2 = d$, as shown in Fig. 2(b). Based on the phenomenological Landau–Devonshire theory, the free energy $U = \frac{\alpha}{2}P^2 + \frac{\beta}{4}P^4 + \frac{\gamma}{6}P^6$ with $\alpha = -39.66$, $\beta = -1.206$, and $\gamma = 2.894$ can be obtained, where U and P are in units of millielectron volts per cell and 10^{-10} C/m, respectively, as shown in Fig. 3(b). The energy barrier E_B between the ferroelectric and paraelectric states can be found to be around 53.3 meV, which is larger than that of the β-GeSe monolayer (11.66 meV). In addition, as shown in Fig. S3 in the supplementary material, a perfect double-well potential vs displacement d along the x direction is also obtained. The energy barrier of such double-well potential is in good agreement with E_B. It is noteworthy that E_B is one order of magnitude smaller than that of other frequently used ferroelectrics such as PbTiO$_3$,[34] suggesting that a rather smaller electric field is required for the polarization reversal.

The ferroelectricity of monolayer β-GeS under applied in-plane biaxial and uniaxial tensile strains is further explored. Figures 3(c) and 3(d) present the strain dependent P_s and E_B of monolayer β-GeS, respectively. Clearly, P_s and E_B increase with increasing in-plane strains, which are attributed to the increase in x direction displacements d_1 and d_2 between adjacent Ge and S atoms. When a 7% biaxial strain is applied, P_s can be enlarged to 2.47×10^{-10} C/m. Thus, T_c of the monolayer β-GeS could be effectively tuned since E_B is of strong strain dependence.

Besides the phenomenological model described above, AIMD simulations are performed to study the phase transition between ferroelectric and paraelectric phases of the β-GeS monolayer. From the AIMD calculations, we can determine the P_s value from the average displacement $\bar{d}$ obtained by using the formula $\bar{d} = \frac{1}{M}\frac{1}{N}\sum_{i=1}^{M}\sum_{j=1}^{N}(d_{ij}^{Ge} - d_{ij}^{S})$, where $(d_{ij}^{Ge} - d_{ij}^{S})$ is the x direction coordinate difference between the nearest neighbor Ge and S ions. M is the number of configuration snapshots extracted from the equilibrium AIMD trajectories (see Fig. S4 in the supplementary material), and N is the number of GeS ion pairs in the supercell. The geometric configurations of the β-GeS monolayer at 100 K, 300 K, and 600 K are shown in Fig. S5 in the supplementary material. Figure 4(a) shows P_s as a function of temperature. At $T = 0$ K, $\bar{d} = 0.306$ Å corresponds to $P_s = 2.00 \times 10^{-10}$ C/m, which is maintained up to about 300 K. The Curie temperature $T_c = 358$ K can be determined by fitting P_s vs temperature T as $P_s(T) = a/(1 + e^{-k(T-T_c)})$, where a and k are constants. The value of T_c is usually influenced by the energy barrier E_B and the dipole-dipole
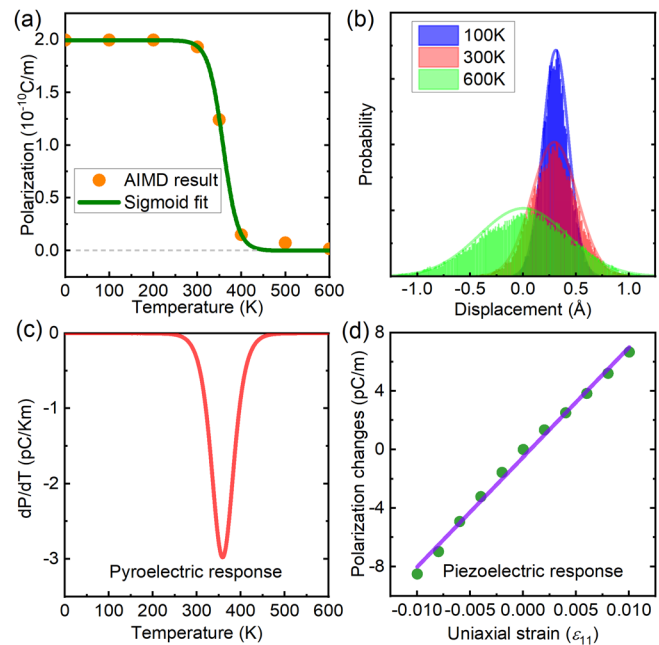

FIG. 4. (a) Temperature dependence of spontaneous polarization obtained from AIMD simulations for the β-GeS monolayer. (b) Thermal evolution of atomic displacements along the x direction between adjacent Ge and S atoms. The data are collected from sampling the AIMD equilibrium structures at 100 K, 300 K, and 600 K, respectively. (c) Pyroelectric coefficient ($-dP/dT$) of the β-GeS monolayer. (d) Piezoelectric response (relaxed-ion e_{11} coefficient) calculated from the DFT method. The polarization and uniaxial strain ε_{11} are all along the x direction. The corresponding relaxed-ion piezoelectric coefficient e_{11} can be obtained from the slope of the line.

interaction among the neighboring unit cells. Compared with another well-studied allotrope of the α-GeS monolayer with $E_B = 580.77$ meV and $T_c = 6400$ K,[12] the obviously smaller $T_c = 358$ K near room temperature for β-GeS could mainly result from its much smaller energy barrier $E_B = 53.3$ meV. Moreover, Fig. 4(b) presents the thermal effects on the in-plane atomic displacements along the x direction, indicating that the probability distribution of displacement strictly obeys a Gaussian function. At low temperature, 100 K, the distribution exhibits a sharp peak with an average displacement $\bar{d}$ of around 0.306 Å, corresponding to a ferroelectric phase. However, with increasing temperature, the peak broadens homogeneously. Near T_c, the broadened peak will shift to the place with an average displacement $\bar{d}$ of around zero, corresponding to a nonpolar phase, which apparently verifies the occurrence of phase transition between ferroelectric and paraelectric phases in the β-GeS monolayer. More importantly, near T_c, the significant broadening of the in-plane atomic displacements along the x direction with a root-mean square (RMS) value close to $\bar{d}$ implies that the soft-mode phonons related to the lattice vibration along the x direction could also be responsible for the relatively low T_c of β-GeS.

The pyroelectric and piezoelectric responses of the β-GeS monolayer are quantitatively determined from the AIMD results.[35] Figure 4(c) shows the pyroelectric coefficient $p = -(dP/dT)$. Near $T_c = 358$ K, p could be as high as 7300 μC/Km^2 when we considered

the effective thickness of 4.12 Å for monolayer β-GeS.[27] Moreover, the piezoelectric coefficient e_{11} is determined by a linear fitting of 2D polarization changes along the x direction with respect to the uniaxial strains ε_{11} along the x direction. As indicated in Fig. 4(d), a linear relation between polarization changes and strains within $\pm 1\%$ has been found for the β-GeS monolayer. The piezoelectric e_{11} coefficient is determined to be about 7.51×10^{-10} C/m, which is twice larger than that of the MoS$_2$ monolayer ($e_{11} = 3.64 \times 10^{-10}$ C/m).[36] The active pyroelectric and piezoelectric responses in the β-GeS monolayer suggest that it has a wide range of applications in sensors and energy conversion devices. Particularly, the giant pyroelectric coefficient is larger than those of most ferroelectric bulk crystals, suggesting that the device containing β-GeS monolayers could have superior pyroelectric performance.

For 2D layered materials, the few-layer nanosheets are easily synthesized and generally applied in device applications. Herein, we have also studied the ferroelectric behavior of few-layer 2D β-GeS. Very similar to β-GeSe nanosheets,[23] the β-GeS nanosheet shown in Fig. 5(a) employs a stacking mode of opposite orientation for alternating monolayers, which is verified to possess the lowest free energy by our theoretical calculation. Figure 5(b) shows P_s as a function of numbers of monolayers N. The 2D β-GeS nanosheets with even numbers of layers could be nonferroelectric because of the existence of inversion symmetry in their structure. In contrast, the spontaneous polarization can arise naturally in the 2D β-GeS nanosheets with odd numbers of monolayers because of the loss of centrosymmetry. Similar N-dependent piezoelectricity has also been discussed and reported in 2D layered materials previously.[37,38] As displayed in Fig. 5(b), P_s can be slightly enhanced in 2D β-GeS nanosheets with odd numbers of monolayers such as trilayer and pentalayer β-GeS. With the rapid development of fabrication techniques, it is quite possible that 2D β-GeS nanosheets could be obtained by exfoliation methods, allowing the applications of 2D β-GeS nanosheets for high-performance sensors, actuators, and energy harvesters.

In summary, 2D ferroelectricity with an in-plane spontaneous polarization in monolayer β-GeS has been predicted by the first-principles DFT calculations, together with AIMD simulations. The spontaneous polarization is larger than those of most reported 2D

ferroelectric materials and can also be enhanced by applied tensile strains. Meanwhile, the ferroelectricity can be maintained in 2D β-GeS nanosheets containing odd numbers of monolayers. As predicted from *ab initio* simulations, the strong polarization (0.49 C/m^2) and giant pyroelectric coefficient (7300 μC/Km^2) at room temperature shed light on the applications of the β-GeS monolayer in sensors, actuators, and energy harvesters with superior performance.

See the supplementary material for the computational details, structural definition of β-phase GeS, comparison of the identical structures of phosphorene and the GeS monolayer in Fig. S1, Berry phase polarization calculation result of the β-GeS monolayer in Fig. S2, double-well potential vs displacements along the x direction in Fig. S3, temperature variations with time in AIMD calculations in Fig. S4, and final geometric configurations of the β-GeS monolayer after performing 5000 fs AIMD simulations in Fig. S5.

REFERENCES

[1] J. Junquera and P. Ghosez, Nature **422**, 506 (2003).

[2] D. D. Fong, G. B. Stephenson, S. K. Streiffer, J. A. Eastman, O. Auciello, P. H. Fuoss, and C. Thompson, Science **304**(5677), 1650–1653 (2004).

[3] N. A. Spaldin, Science **304**(5677), 1606 (2004).

[4] C. Tan, X. Cao, X.-J. Wu, Q. He, J. Yang, X. Zhang, J. Chen, W. Zhao, S. Han, G.-H. Nam, M. Sindoro, and H. Zhang, Chem. Rev. **117**(9), 6225–6331 (2017).

[5] S. N. Shirodkar and U. V. Waghmare, Phys. Rev. Lett. **112**(15), 157601 (2014).

[6] K. Chang, J. Liu, H. Lin, N. Wang, K. Zhao, A. Zhang, F. Jin, Y. Zhong, X. Hu, W. Duan, Q. Zhang, L. Fu, Q.-K. Xue, X. Chen, and S.-H. Ji, Science **353**(6296), 274 (2016).

[7] F. Liu, L. You, K. L. Seyler, X. Li, P. Yu, J. Lin, X. Wang, J. Zhou, H. Wang, H. He, S. T. Pantelides, W. Zhou, P. Sharma, X. Xu, P. M. Ajayan, J. Wang, and Z. Liu, Nat. Commun. **7**, 12357 (2016).

[8] Y. Zhou, D. Wu, Y. Zhu, Y. Cho, Q. He, X. Yang, K. Herrera, Z. Chu, Y. Han, M. C. Downer, H. Peng, and K. Lai, Nano Lett. **17**(9), 5508–5513 (2017).

[9] C. Cui, W.-J. Hu, X. Yan, C. Addiego, W. Gao, Y. Wang, Z. Wang, L. Li, Y. Cheng, P. Li, X. Zhang, H. N. Alshareef, T. Wu, W. Zhu, X. Pan, and L.-J. Li, Nano Lett. **18**(2), 1253–1258 (2018).

[10] C. Zheng, L. Yu, L. Zhu, J. L. Collins, D. Kim, Y. Lou, C. Xu, M. Li, Z. Wei, Y. Zhang, M. T. Edmonds, S. Li, J. Seidel, Y. Zhu, J. Z. Liu, W.-X. Tang, and M. S. Fuhrer, Sci. Adv. **4**(7), eaar7720 (2018).

[11] D. Di Sante, A. Stroppa, P. Barone, M.-H. Whangbo, and S. Picozzi, Phys. Rev. B **91**(16), 161401 (2015).

[12] R. Fei, W. Kang, and L. Yang, Phys. Rev. Lett. **117**(9), 097601 (2016).

[13] W. Wan, C. Liu, W. Xiao, and Y. Yao, Appl. Phys. Lett. **111**(13), 132904 (2017).

[14] B. Xu, H. Xiang, Y. Xia, K. Jiang, X. Wan, J. He, J. Yin, and Z. Liu, Nanoscale **9**(24), 8427–8434 (2017).

[15] S.-H. Zhang and B.-G. Liu, Nanoscale **10**(13), 5990–5996 (2018).

[16] S. Guan, C. Liu, Y. Lu, Y. Yao, and S. A. Yang, Phys. Rev. B **97**(14), 144104 (2018).

[17] C. Xiao, F. Wang, S. A. Yang, Y. Lu, Y. Feng, and S. Zhang, Adv. Funct. Mater. **28**(17), 1707383 (2018).

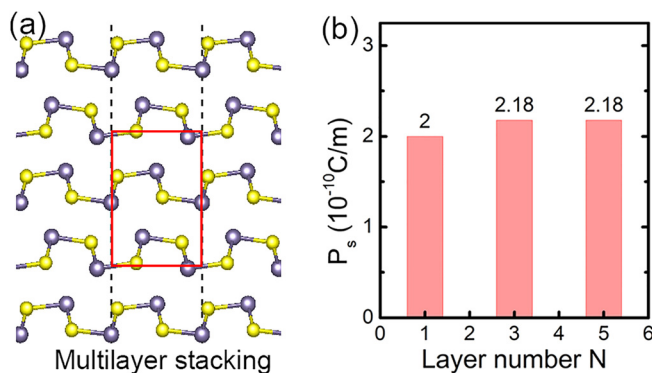[18] C. Liu, W. Wan, J. Ma, W. Guo, and Y. Yao, Nanoscale **10**(17), 7984–7990 (2018).

FIG. 5. (a) Stacking mode of multilayer β-GeS. This stacking structure is similar to that of multilayer β-GeSe obtained in experiment.[23] The red rectangle denotes the unit cell of β-GeS bulk. (b) Spontaneous polarizations P_s of layered β-GeS as a function of the layer number N.

[19]J. Liu and S. T. Pantelides, Phys. Rev. Lett. **120**(20), 207602 (2018).

[20]J. Liu and S. T. Pantelides, 2D Mater. **6**(2), 025001 (2019).

[21]H. Aziguli, X. Chen, Y. Liu, G. Yang, P. Yu, and Q. Wang, Appl. Phys. Lett. **112**(19), 193902 (2018).

[22]F. Zhuo, Q. Li, H. Qiao, Q. Yan, Y. Zhang, X. Xi, X. Chu, X. Long, and W. Cao, Appl. Phys. Lett. **112**(13), 133901 (2018).

[23]F. O. von Rohr, H. Ji, F. A. Cevallos, T. Gao, N. P. Ong, and R. J. Cava, J. Am. Chem. Soc. **139**(7), 2771–2777 (2017).

[24]G. Kresse and J. Furthmüller, Phys. Rev. B **54**(16), 11169–11186 (1996).

[25]G. Kresse and J. Furthmüller, Comput. Mater. Sci. **6**(1), 15–50 (1996).

[26]G. Kresse and D. Joubert, Phys. Rev. B **59**(3), 1758–1775 (1999).

[27]N. Luo, C. Wang, Z. Jiang, Y. Xu, X. Zou, and W. Duan, Adv. Funct. Mater. **28**(46), 1804581 (2018).

[28]S. Zhang, M. Xie, F. Li, Z. Yan, Y. Li, E. Kan, W. Liu, Z. Chen, and H. Zeng, Angew. Chem. Int. Ed. **55**(5), 1666–1669 (2016).

[29]G. Wang, R. Pandey, and S. P. Karna, ACS Appl. Mater. Interfaces **7**(21), 11490–11496 (2015).

[30]Z.-Y. Hu, K.-Y. Li, Y. Lu, Y. Huang, and X.-H. Shao, Nanoscale **9**(41), 16093–16100 (2017).

[31]T. Hu and J. Dong, Phys. Chem. Chem. Phys. **18**(47), 32514–32520 (2016).

[32]K. S. Novoselov, A. K. Geim, S. V. Morozov, D. Jiang, Y. Zhang, S. V. Dubonos, I. V. Grigorieva, and A. A. Firsov, Science **306**(5696), 666 (2004).

[33]L. Li, Y. Yu, G. J. Ye, Q. Ge, X. Ou, H. Wu, D. Feng, X. H. Chen, and Y. Zhang, Nat. Nanotechnol. **9**, 372 (2014).

[34]R. E. Cohen, Nature **358**(6382), 136–138 (1992).

[35]D. Damjanovic, Rep. Prog. Phys. **61**(9), 1267–1324 (1998).

[36]K.-A. N. Duerloo, M. T. Ong, and E. J. Reed, J. Phys. Chem. Lett. **3**(19), 2871–2876 (2012).

[37]K. H. Michel and B. Verberck, Phys. Rev. B **83**(11), 115328 (2011).

[38]W. Wu, L. Wang, Y. Li, F. Zhang, L. Lin, S. Niu, D. Chenet, X. Zhang, Y. Hao, T. F. Heinz, J. Hone, and Z. L. Wang, Nature **514**, 470 (2014).